

## DEGRADATION OF CONCRETE-BASED STRUCTURES BY ATMOSPHERIC AND ENVIRONMENTAL FACTORS: A FAST AND VERSATILE ON-SITE MONITORING APPROACH

DOMENICO LOMBARDO <sup>a\*</sup>, MARIA TERESA CACCAMO <sup>bc</sup>,  
ALESSANDRO BONCALDO <sup>bd</sup> EMANUELE CALABRÒ <sup>c</sup>, GIUSEPPE COLLORÀ <sup>ab</sup>,  
SALVATORE MAGAZÙ <sup>bcd</sup> ROBERTO CARUSO <sup>a</sup>, GIUSEPPE LUPÒ <sup>a</sup>,  
GUERINO SARULLO <sup>a</sup> AND GIUSEPPE SPINELLA <sup>a</sup>

**ABSTRACT.** We present a preliminary study on a fast and versatile approach, based on the use of a portable Raman spectrometer, for the on-site monitoring of the degradation of concrete-based structures by atmospheric and environmental factors. The main results of our investigation evidence that most of the amorphous and crystal materials involved in Carbonation and Sulphate Attack (the main deterioration processes of cement-based materials) can be detected and distinguished with the use of the Raman spectroscopy. The main wave numbers and changes in the relevant chemical phases ( $\text{CO}_3^{2-}$ ,  $\text{SiO}_4^{2-}$ ,  $\text{SO}_4^{2-}$  etc.) which generally occur under these durability attacks were discussed and summarized. The proposed approach may open new perspectives in the field of structural health monitoring and suggests a powerful instrument to investigate the relevant processes connected with the degradation processes (and the underlying chemical reactions) caused by atmospheric and environmental factors.

### 1. Introduction

Concrete-based structures (and infrastructures) are the predominant type of constructions worldwide. Their performance during the time is therefore crucial to ensure the essential economic activities and services that they intend to support (Neville 1995). Although the rate of deterioration of constructions strongly depends on the construction processes and the employed material components, the deterioration process is also intimately connected with the atmospheric, environmental and climatic factors encountered during the construction service lifecycle (Yoon, Copuroglu, and Ki-Bong 2007). More specifically, carbon concentration, increase in temperature (due to the global warming) and the change of humidity are among the main factors that negatively influence the duration, serviceability and safety of concrete-based structures (Qu *et al.* 2021; Bastidas-Arteaga *et al.* 2022; Castorina *et al.* 2022). As it is well-known, the concentration of atmospheric  $\text{CO}_2$  is strongly increasing at the global scale, due to the uncontrolled increase of anthropic activities. This increase

of CO<sub>2</sub> (together with other climate altering gases) cause also a correlated increase in air temperature (about 1°C compared to the preindustrial era) at the global scale. Finally, a third important environment factor is given by the atmospheric humidity, which evolutions is affected by local conditions (such as the orography, sea distance and urban environment) (Yoon, Copuroglu, and Ki-Bong 2007; Bastidas-Arteaga *et al.* 2022). In Table 1, we report the main changes of atmospheric, environment and climate factors that influence the durability of concrete (infra-)structures

TABLE 1. Principal modifications of atmospheric, environmental, and climatic factors influencing the durability of concrete (infra-)structures.

<b>Atmospheric, environmental and climatic factors</b>	<b>Consequences</b>
It increase of carbon concentration	It accelerates the carbonation process and increases carbonation depth in concrete structures (structural damage). It increases carbonation-induced reinforcement corrosion initiation in reinforced concrete structures.
Temperature increase (Global warming)	An increase in temperature accelerates the carbonation process, sulphate attack, chloride penetration, and the corrosion rate of reinforced structures.
Change of humidity	A decrease in relative humidity (RH) may reduce carbonation and sulphate attack, while an increase in humidity favours carbonation, chloride, and sulphate attack.

As evidenced in Table 1, carbonation, chloride and sulphate attacks represent the main outcome produced by the atmospheric and environmental factors. However, the severity of the deterioration effects in the constructions vary significantly from place to place and over the time. For this reason a precise determination of the impact of the carbonation-induced corrosion and sulphate/chloride attack on the concrete structures require a large scale investigation on numerous (infra-)structures by means of accurate laboratory tests. A *large scale (regional) mapping* of the those phenomena represents a first step for the comprehension of the the main atmospheric and environmental factors influencing the degradation of Concrete-based structures (as a function of time) at various spatial scales, *e.g.*, city, region, country, etc. . . (Rouainia *et al.* 2020; Castorina *et al.* 2022)

Within this context, the main goal of this work is to propose a smart and rapid approach, based on the use of a portable Raman spectrometer, for the on-site monitoring of the carbonation and sulphate attach processes on reinforced concrete structures. The identification of a smart and relatively economic tool for a fast (on-site) monitoring of the extent the degradation in a relevant number of reinforced concrete structures allow a fast monitoring and a better evaluation on concrete endurance and the prediction of the service life of the (infra-)structures at various spatial scales (*e.g.*, city, region, country, etc.) (Geiker, Hendriks, and Elsener 2023).

## 2. In situ structure monitoring by means of portable Raman technology

The on-site measurements (and tests) of the chemical changes of concrete-based structures play an important role in the structure health monitoring as it provide crucial information about the cause (and evolution) of the degradation mechanisms of structures, thus furnishing valuable information for the diagnosis of the health condition and performance of concrete-based structures. For these reasons, there is an increasing interest in the design and development of smart sensor systems for the (on-site) monitoring the chemical environment of concrete, as well as to obtain non-destructive (and time dependent) information concerning the condition of concrete structure (Shevtsov *et al.* 2022). Some of the recent efforts are aimed at the identification of non-destructive monitoring methods and/or continuous monitoring systems based on electrochemical (Rodrigues *et al.* 2021), piezoelectric (Thakur 2022), fiber-optic (Fan and Bao 2021), control of chloride content (Robles, Yee, and Kee 2022) approaches. However, these approaches have not yet provided prototypes ready to be placed on the market.

Spectroscopic and scattering techniques have long provided a formidable tool for the analysis and characterization of materials in their complex aggregative states (Gierlinger and Schwanninger 2007; Gastaldi *et al.* 2010; M. T. Caccamo *et al.* 2020; Lombardo, Calandra, and Kiselev 2020; Simonpietro 2021), as well as a useful tool for investigating self-assembly processes in a wide range of space-time resolution of nanostructured systems in the field of materials science and engineering (Bonaccorsi *et al.* 2009, 2013a,b; Narayanan and Konovalov 2020; Wagatsuma 2021). These spectroscopic techniques are commonly employed not just for species identification but also for acquiring precise structural data, including bond lengths, bond angles, and flow analysis (Faraone *et al.* 1999; Magazù, Migliardo, and Benedetto 2011; Magazù *et al.* 2013; M. T. Caccamo *et al.* 2017; M. T. Caccamo and Magazù 2017b).

More specifically, Raman scattering provide a unique opportunity for developing a novel approach capable of monitoring the service-condition of concrete (Long 1977; Colomban and Slodczyk 2010; Martinez-Ramirez and Fernandez-Carrasco 2010). Raman spectroscopy is able to detect the rotational and vibrational modes (of the chemical bonds) of molecules inside a material system, by using specific laser wavelengths which are not absorbed by the material sample under investigation. More specifically, one of the most important characteristic of the Raman technique is its ability to perform in-situ (real-time) analysis (Martinez-Ramirez and Fernandez-Carrasco 2010; Ševčík and Mácová 2018; Yue *et al.* 2018). Moreover, Raman spectroscopy has attracted increasing interest for the investigation of various phases in concrete-based structures due to its unique capability to investigate various environmental attacks like carbonation (Martinez-Ramirez *et al.* 2003; Black *et al.* 2007; Ševčík and Mácová 2018; Yue *et al.* 2018; Tang, Ling, and Mo 2021) and sulfate attack (Sahu, Exline, and Nelson 2002; Irassar, Bonavetti, and González 2003; Yue *et al.* 2013).

In this study, the concrete deterioration of reinforced concrete samples subjected to multi-environmental factors are investigated by means of portable Raman spectroscopy set-up. More specifically, we provide an overview of the use of portable Raman spectroscopy in the characterization of carbonate, sulfate, and silicate phases to study carbonation, sulfate attacks on cement-based materials. Raman spectra were collected by using a Bruker BRAVO

equipment, in the 300-3200  $\text{cm}^{-1}$  range. The instrument uses SSETM (Sequentially Shifted Excitation) a patented fluorescence mitigation method that permits to measure a much extensive range of materials with handheld Raman setup. Samples were excited by using two lasers centred at 785 and 853 nm working together, in order to mitigate the fluorescence phenomena and offering highest sensitivity across the entire spectral range.

**2.1. Carbonation Degradation Process.** Amongst various environmental and chemical deterioration mechanisms influencing the durability of concrete structures, carbonation is probably the most important action. This mechanism occurs from the chemical reactions between intruded  $\text{CO}_2$  and calcium-bearing phases, and involves the reaction of carbon dioxide ( $\text{CO}_2$ ) with alkaline ions from the pore solution. Most phases in hydrated cement paste can react with  $\text{CO}_2$ , to convert the calcium ions ( $\text{Ca}^{2+}$ ) from cement paste to calcium carbonate ( $\text{CaCO}_3$ ). This process favours the formation of calcium carbonate ( $\text{CaCO}_3$ ) followed by the decrease of the alkalinity of concrete pore solution, thus causing the corrosion of the rebar in concrete (Masmoudi *et al.* 2017). Thus, detecting carbonation process, by determining the carbonation products formed against the depth into concrete structure, is of great importance to the diagnosis of the health condition of concrete-based structures and the prediction of their service life. Traditional methods used to evaluate carbonation process in cement-based materials, such as Phenolphthalein spray test, x-rays diffraction (XRD), thermogravimetric analysis (TGA), mercury intrusion porosimetry (MIP) often require a complex sample preparation, and the sample need to be taken (extracted) from the (infra-)structures (Balachandran, Muñoz, and Arnold 2017). These approaches are time-consuming and can severely damage the structural features of cementitious samples under investigation. Raman spectroscopy technique can be employed in-situ, without causing the damage the micro-structure of the reference material sample.

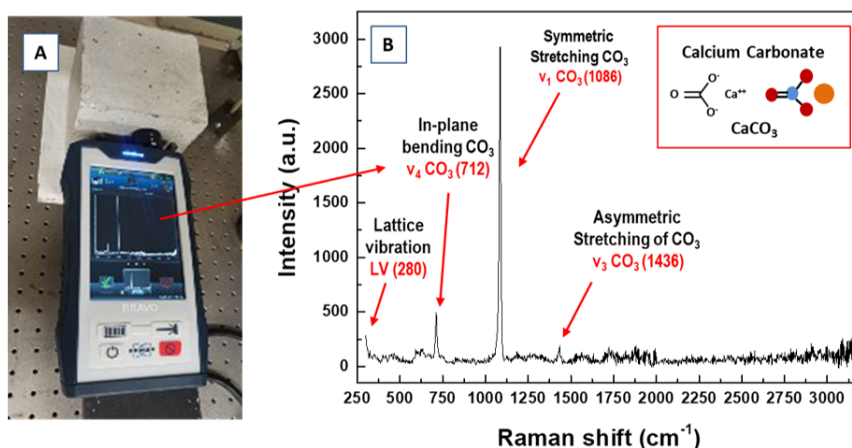


FIGURE 1. Portable Raman setup and Raman spectrum on a concrete cubic (150x150x150 mm) specimen showing typical characteristic peaks and associated  $\text{CaCO}_3$  vibrational bands (modes), and the assignments corresponding to the Calcite phase (red).

In Figure 1, we report the main features of a test performed with the portable Raman setup (BRAVO-Bruker) on a cubic concrete specimen (150x150x150 mm). The recorded Raman spectrum evidence the presence of the typical characteristic peaks and associated vibrational bands (modes) of calcium carbonate ( $\text{CaCO}_3$ ). This spectrum is dominated by a pronounced and intense peak (located in the range from 1076 to 1090  $\text{cm}^{-1}$ ), which is characteristic of the  $\nu$  symmetric stretching band of the  $\text{CO}_3$  groups, and by three minor bands which can be attributed to the Ca-O lattice vibration [LV] ( $< 350 \text{ cm}^{-1}$ ), the in-plane bending [ $\nu_4$ ] (700–750  $\text{cm}^{-1}$ ) and the asymmetric stretching vibration [ $\nu_3$ ] ( $\nu_3=1436 \text{ cm}^{-1}$ , for the Calcite)(Yue *et al.* 2018). The  $\text{CO}_3$  phases precipitated within the concrete-based structures could exist in three different polymorphs, namely Calcite (a thermodynamically stable, well-crystallised phase) and Vaterite and Aragonite (less stable, poor-crystallised, phases) (Tang, Ling, and Mo 2021). The less thermodynamically stable Vaterite and Aragonite will undergo to a gradual transformation in Calcite. The Raman spectroscopy technique is highly effective in distinguishing among those phases by the analysis of the spectral peaks position. In Figure 1, we reported the position of the characteristic peaks of the Calcite phase (namely  $\nu_1=1086 \text{ cm}^{-1}$ , LV=280 $\text{cm}^{-1}$ ,  $\nu_4=712 \text{ cm}^{-1}$ ,  $\nu_3=1436 \text{ cm}^{-1}$ ) (Yue *et al.* 2018). Similarly, characteristic peaks assignments can be associated also to the phases of Vaterite ( $\nu_1=1076/1090 \text{ cm}^{-1}$ , LV=280  $\text{cm}^{-1}$ ,  $\nu_4=712 \text{ cm}^{-1}$ ) and Aragonite (namely  $\nu_1=1085 \text{ cm}^{-1}$ , LV=206  $\text{cm}^{-1}$ ,  $\nu_4=701/704 \text{ cm}^{-1}$ ) (Black *et al.* 2007; Tang, Ling, and Mo 2021). Generally, the content of  $\text{CO}_3$  (degree of carbonation) decreases with increasing distance from the exposed surface of concrete, due to the reduced penetration of environment  $\text{CO}_2$  into the interior part of concrete sample. This cause a decrease of the peak height with the increase of the carbonation depth of the most intense peak of the carbonates (*i.e.* the  $\nu_1(\text{CO}_3)$  symmetric stretching band). This peak height can be used as an indicator to quantify the amount of carbonates formed in concrete samples, by comparing this parameter with a TG analysis used for a preliminary quantification of the calcium carbonate (used as calibration reference) (Yue *et al.* 2018). Finally, it is worth noticing that the Raman peak  $\nu_1(\text{CO}_3)$  (at 1086  $\text{cm}^{-1}$  for Calcite) is very close to that of the  $\nu_1(\text{SiO}_4^{2-})$  of Q3 tetrahedra located at 1080  $\text{cm}^{-1}$ , thus causing a sensitive overlap between these two different minerals.

**2.2. Sulphate attack.** Sulfate attack is a complex physical-chemical process that causes the alterations to concrete. Absorption of sulfates (and moisture) from the external environment favours multiple complex chemical reactions between sulfate ion-bearing water and cement hydration products, and give rise to the formation of Gypsum ( $\text{CaSO}_4 \cdot 2\text{H}_2\text{O}$ ), Ettringite ( $6\text{CaO} \cdot \text{Al}_2\text{O}_3 \cdot 3\text{SO}_3 \cdot 32\text{H}_2\text{O}$ ), Thaumasite ( $\text{CaCO}_3 \cdot \text{CaSO}_4 \cdot \text{CaSiO}_3 \cdot 15\text{H}_2\text{O}$ ), and an alteration of the structure of the calcium silicate hydrate (C-S-H) gel (Irassar, Bonavetti, and González 2003; Yue *et al.* 2013). Formation of those products is considered to be the primary process for the sulfate attack damage, and is manifested in the form of expansion, surface softening and spalling, and overall loss of cohesiveness and mechanical properties of the concrete. It is worth pointing that, while for the monitoring on site of the carbonation and chloride attack the development of some electrical-resistance and fiber optic chemical sensors are under investigation, currently there is no detection system for the on site monitoring of the deterioration actions of sulfate attack.

In Figure 2 A-C, we report the main structural features of a reinforced concrete retaining wall, which has undergone a significant degradation effect due to atmospheric and environmental factors (including CO<sub>2</sub>, water and humidity infiltrations, temperature variations). In Figure 2D we report the corresponding Raman spectrum obtained by using the portable Raman setup Bravo-Bruker. Generally, the Raman spectrum of a degraded cement-base structure present a given degree of complexity which is connected with the complex overlap of multiple degradation events (and their relevant phases). However, as the chemical group SO<sub>4</sub><sup>2-</sup> is found to be Raman active (possessing 4 vibration modes  $\nu_1 - \nu_4$  (SO<sub>4</sub><sup>2-</sup>)), it is possible to use the Raman spectroscopy to distinguish between the relevant phases for an (in-situ) monitoring the sulfate attack. For this reason it is very important to compare the spectra obtained from (on site) Raman measurements with the experimental results obtained on (reference) pure samples of Gypsum, Ettringite and Thaumassite.

In this respect, a previous investigation [33] evidenced that pure Gypsum has four major Raman peaks, ranging from the symmetric stretching  $\nu_1$  [SO<sub>4</sub><sup>2-</sup>] (at 1006 cm<sup>-1</sup>), the symmetric bending  $\nu_2$  [SO<sub>4</sub><sup>2-</sup>] (at 415 cm<sup>-1</sup> and 435 cm<sup>-1</sup>), the asymmetric stretching  $\nu_3$  [SO<sub>4</sub><sup>2-</sup>] (at 1135 cm<sup>-1</sup>), and the asymmetric bending  $\nu_4$  [SO<sub>4</sub><sup>2-</sup>] (at 620 cm<sup>-1</sup> and 670 cm<sup>-1</sup>).

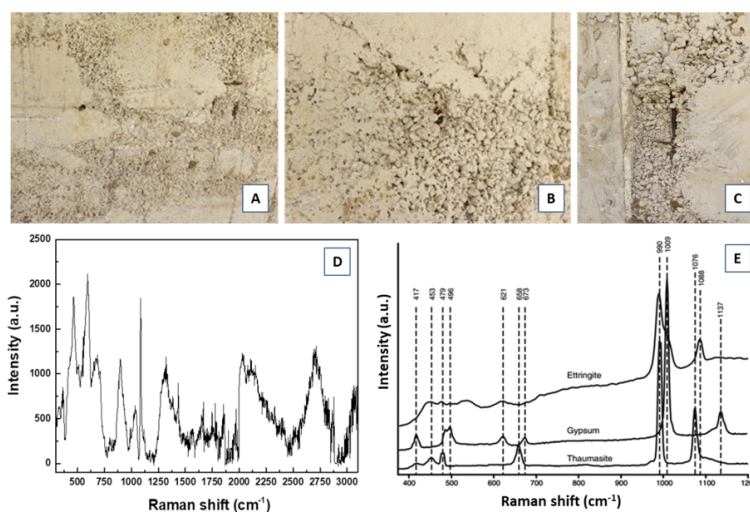


FIGURE 2. Example of the main structural features of a reinforced concrete retaining wall, exhibiting a significant degradation effect due to environmental factors (A-C), and corresponding Raman spectrum obtained by using the portable Raman spectrometer (D). Summary of the main characteristic bands of Raman spectra of Gypsum, Ettringite and Thaumassite (From Sahu, Exline, and Nelson 2002).

In Table 2 are reported the main Raman bands and assignments of pure gypsum and ettringite under bench-mounted Raman spectroscopy (Yue *et al.* 2013). Apart from the Gypsum and Ettringite, the sulfate attack from the Thaumassite phase has been recognized

TABLE 2. Raman bands and assignments of pure Gypsum and Ettringite under bench-mounted Raman spectroscopy (Yue *et al.* 2013).

Raman Shift (cm <sup>-1</sup> )		Vibrational Bands
Gypsum	Ettringite	
1008	988	$\nu_1$ symmetric stretching of (SO <sub>4</sub> )
414, 493	448	$\nu_2$ symmetric bending of (SO <sub>4</sub> )
1136	1119	$\nu_3$ asymmetric stretching of (SO <sub>4</sub> )
618, 670	612	$\nu_4$ asymmetric stretching of (SO <sub>4</sub> )

to be particularly deleterious and more severe than the other forms, because its reaction products transform the surface of the concrete into a soft pulpy mass. Raman spectra of Thaumasite evidences three strong peaks at  $\nu_1$ [SiO<sub>6</sub>] (658 cm<sup>-1</sup>),  $\nu_1$ [SO<sub>4</sub><sup>2-</sup>] (990 cm<sup>-1</sup> and 1076 cm<sup>-1</sup>), and four weak bands at symmetric bending of  $\nu_2$  (SO<sub>4</sub><sup>2-</sup>) (at 417, 453, 479 cm<sup>-1</sup>) and at 3300 cm<sup>-1</sup> (Sahu, Exline, and Nelson 2002; Irassar, Bonavetti, and González 2003; Black *et al.* 2007; Yue *et al.* 2013). A summary of the main characteristic of Raman spectra of Gypsum, Ettringite and Thaumasite is reported in Figure 2E (Sahu, Exline, and Nelson 2002).

In Figure 3 we report the analysis (assignments) of main characteristic bands of Gypsum (green) and Ettringite (red) of a reinforced concrete retaining wall, obtained (on site) by using the portable Raman system (Bravo-Bruker). It is worth noticing that despite the complexity of the recorded Raman spectrum (which is connected with the complexity of multiple overlapping degradation events) the Raman spectroscopy allow to clearly identify the relevant phases of the sulfate attack.

Raman spectroscopy can provide also important information concerning the water molecules changes within the cement (and concrete) matrix (Masmoudi *et al.* 2017). More specifically, the water inside cement-based materials can be divided into bound water (involved in the cement hydration reaction) and free water (that does not participate in hydration), and is identified by broad Raman peak between 3200 and 3600 cm<sup>-1</sup>). Finally, since Raman technique is sensitive to less-crystalline structures, it has been experimented in the investigation of the time evolution gels products of ASR, a chemical reaction occurring between poorly crystalline (or amorphous) silica in aggregates and alkaline pore solution of concrete (Balachandran, Muñoz, and Arnold 2017; Shi *et al.* 2019).

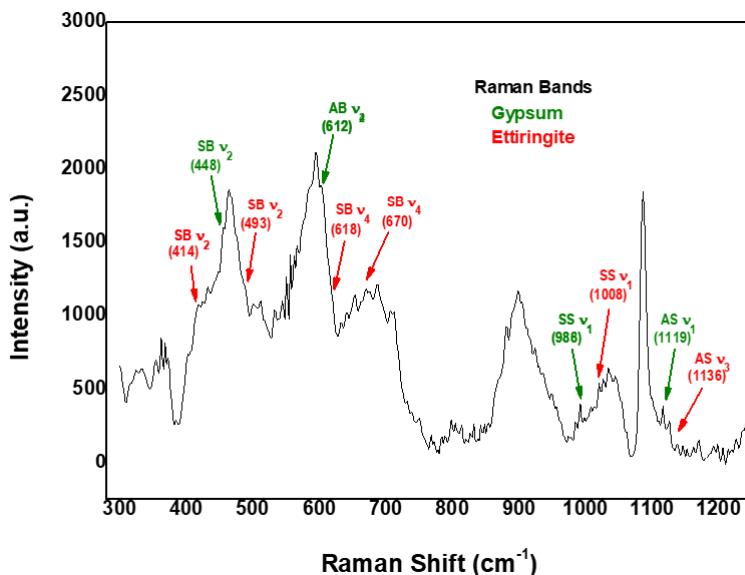


FIGURE 3. On site Raman spectrum (using the portable Raman spectrometer) of a reinforced concrete retaining wall, with the indication of the main characteristic bands of Gypsum (green) and Ettringite (red).

**2.3. Use of Complementary Techniques (Fourier Transform Infrared Spectroscopy - FTIR).** Because of the complexity of the processes involved in the degradation of the concrete-based materials, very often it is necessary to employ complementary techniques for an exhaustive characterization of the degree of deterioration of materials and to understand its effects on the properties and integrity of the structures. In this context, Fourier Transform Infrared (FTIR) spectroscopy represent a powerful technique that allow a versatile (non-destructive) complementary investigation, capable of evaluating (in a qualitative or semi-quantitative way) both amorphous and crystalline materials, and to evaluate hydration or carbonation products of cement-based materials (Valliant *et al.* 2016; Jose *et al.* 2020). In Figure 4, we report the FTIR spectra of the reinforced concrete retaining wall, with the indication of the detected main characteristic bands.

From the FTIR spectral profile it is possible to describe the following characteristics:

- (A) the presence of a weak peak at  $3640\text{ cm}^{-1}$  related to the OH stretching of portlandite (CH),
- (B) a broad band at the  $3000\text{-}3700\text{ cm}^{-1}$  range, attributed to the OH stretching of the water (within the cement matrix),
- (C) a small peak at  $1640\text{ cm}^{-1}$ , attributed to bending vibration of water in sulfates,
- (D) the carbonate ( $\text{CO}_3^{2-}$ ) peaks at  $1410\text{ cm}^{-1}$  (asymmetric C-O stretching),  $873\text{ cm}^{-1}$  (out-of-plane vibration), and  $713\text{ cm}^{-1}$  (in-plane vibration), associated with calcite ( $\text{CaCO}_3$  polymorph),

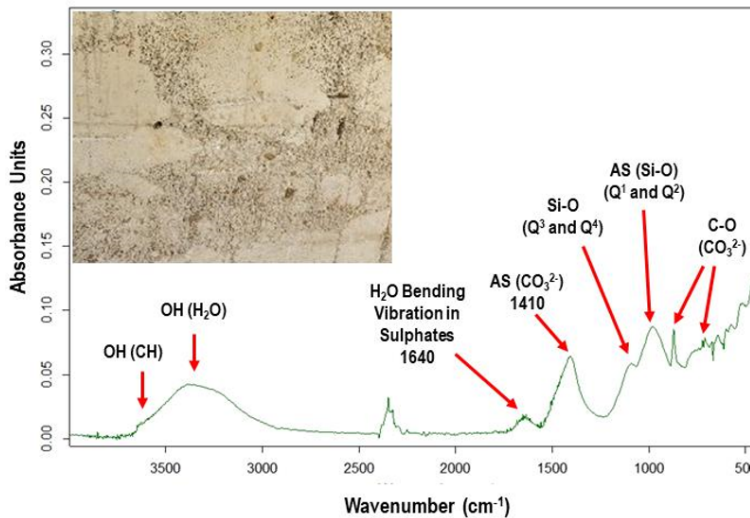


FIGURE 4. FTIR spectra of a degraded (reinforced concrete) retaining wall, with the indication of the main characteristic vibrational bands detected.

- (E) a broad band ( $800\text{--}1100\text{ cm}^{-1}$ ), centered at  $960\text{ cm}^{-1}$ , assigned to the Si-O asymmetric stretching ( $\nu_3$ ) of Q1 and Q2 species of calcium silicate hydrate (C-S-H) (Zhan *et al.* 2018; Skocek, Zajac, and Ben Haha 2020; Higl *et al.* 2021),
- (F) a band ( $1000\text{--}1250\text{ cm}^{-1}$ ), weakly centered at  $1140\text{ cm}^{-1}$  and  $1050\text{ cm}^{-1}$ , that can be assigned to the Si-O asymmetric stretching ( $\nu_3$ ) of the decalcified C-S-H (Q3 at  $1050\text{ cm}^{-1}$ ) and polymerized silica (Q4 at  $1140\text{ cm}^{-1}$ ) phases (Hidalgo *et al.* 2008; Skocek, Zajac, and Ben Haha 2020; Saillio *et al.* 2021).

The analysis of the FTIR spectra confirms the main features of the Raman spectroscopy results and indicates the total consumption of CH by the weakening of the typical OH stretching band at  $3640\text{ cm}^{-1}$ , with the formation of Calcite, evidenced by the visible carbonate ( $\text{CO}_3^{2-}$ ) peaks at  $1410\text{ cm}^{-1}$  (asymmetric C-O stretching),  $873\text{ cm}^{-1}$  (out-of-plane vibration) and  $713\text{ cm}^{-1}$  (in-plane vibration). Moreover, the contemporary presence of the Si-O asymmetric stretching ( $\nu_3$ ) centered at  $960\text{ cm}^{-1}$ , (typical of non-carbonated cement) and the band centered at  $1140\text{ cm}^{-1}$  and  $1050\text{ cm}^{-1}$  (typical of carbonated samples) (Hidalgo *et al.* 2008), indicate the partial consumption of Q1 and Q2 species of calcium silicate hydrate (C-S-H) of non-carbonated cement by the carbonation process, resulting in a decalcification-polymerization process of C-S-H (Q1 and Q2) and leading to the production of decalcified C-S-H (Q3) and polymerized silica (Q4) phases (Saillio *et al.* 2021). In summary, the spectroscopic and scattering techniques represent powerful methods that investigate the structural ordering and phase transitions brought about by the relevant parameters of materials systems such as chemical reactivity and polydispersity, surface charge density, nanoparticle volume fraction, and can be considered as pivotal techniques to investigate in a wide range of material systems (Magazù *et al.* 1989; Lombardo 2009; Gordon *et al.* 2013; M. T. Caccamo and Magazù 2017a; C. Chen *et al.* 2017; Lombardo *et al.*

2019). Furthermore, those techniques allow to obtain important information concerning the collective modes and interactions in material systems, thus allowing the modeling of the main synergistic interactions that regulate the (colloidal) stability and phase transition in complex supramolecular aggregates (Micali *et al.* 1998; S. Chen *et al.* 2002; Zemb and Lindner 2002; Lee 2008; Narayanan and Konovalov 2020; Anker *et al.* 2023).

### 3. Conclusions and Future Perspectives

As severity of constructions deterioration by atmospheric and environmental factors vary significantly from place to place and over the time (Jouzel *et al.* 1987; M. T. Caccamo and Magazù 2019; Castorina, M. T. Caccamo, and Magazù 2019; Lacasse, Gaur, and Moore 2020; Castorina *et al.* 2021; Magazù and M. Caccamo 2022; M. T. Caccamo and Magazù 2023), a precise determination of its impact on structures requires a large scale investigation (and mapping) on numerous (infra-)structures by means of a smart and rapid on-site monitoring approach. Our study shows a potential for the use of portable Raman spectroscopy system for the on-site monitoring of the degradation processes (namely carbonatation and sulphate attack) on reinforced concrete-based structures. With the use of Raman spectroscopy, we evidenced that most of the crystal and amorphous materials involved in the deterioration reactions of cement-based materials can be detected and distinguished by their specific molecular structure. The main wave numbers and changes in chemical phases ( $\text{CO}_3^{2-}$ ,  $\text{SiO}_4^{2-}$ ,  $\text{SO}_4^{2-}$  etc.) which generally occur under these durability attacks were discussed and summarized. The use of the portable Raman system represents then a smart method for a (on-site) fast monitoring of the degradation of reinforced concrete structures for a better evaluation of the service life of a numerous (infra-)structures. It also represents a powerful tool to study the relevant mechanisms and processes connected with the degradation processes caused by atmospheric and environmental factors.

### Acknowledgments

This research was supported by the Ministero dello Sviluppo Economico under Grant No. F/190188/02/X44 - PON I&C 2014-2020, "Sviluppo e ottimizzazione di un sistema general purpose modulare per il monitoraggio strutturale" (MONVIA).

### References

- Anker, A. S., Butler, K. T., Selvan, R., and Jensen, K. M. Ø. (2023). "Machine learning for analysis of experimental scattering and spectroscopy data in materials chemistry". *Chemical Science*. **14**, 14003–14019. DOI: [10.1039/D3SC05081E](https://doi.org/10.1039/D3SC05081E).
- Balachandran, C., Muñoz, J. F., and Arnold, T. (2017). "Characterization of alkali silica reaction gels using Raman spectroscopy". *Cement and Concrete Research* **92**, 66–74. DOI: [10.1016/j.cemconres.2016.11.018](https://doi.org/10.1016/j.cemconres.2016.11.018).
- Bastidas-Arteaga, E., Rianna, G., Gervasio, H., and Nogal, M. (2022). "Multi-region lifetime assessment of reinforced concrete structures subjected to carbonation and climate change". *Structures* **45**, 886–899. DOI: [10.1016/j.istruc.2022.09.061](https://doi.org/10.1016/j.istruc.2022.09.061).
- Black, L., Breen, C., Yarwood, J., Garbev, K., Stemmermann, P., and Gasharova, B. (2007). "Structural features of C-S-H(I) and its carbonation in air – a Raman spectroscopic study. Part II: carbonated

- phases”. *Journal of the American Ceramic Society* **90**, 908–917. DOI: [10.1111/j.1551-2916.2006.01429.x](https://doi.org/10.1111/j.1551-2916.2006.01429.x).
- Bonaccorsi, L., Calandra, P., Amenitsch, H., Proverbio, E., and Lombardo, D. (2013a). “Growth of fractal aggregates during template directed SAPO-34 zeolite formation”. *Microporous and Mesoporous Materials* **167**, 3–9. DOI: [10.1016/j.micromeso.2012.10.024](https://doi.org/10.1016/j.micromeso.2012.10.024).
- Bonaccorsi, L., Calandra, P., Kiselev, M., Proverbio, E., and Lombardo, D. (2013b). “Self-assembly in poly(dimethylsiloxane)-poly(ethylene oxide) block copolymer template directed synthesis of linde type A zeolite”. *Langmuir* **29**, 7079–7086. DOI: [10.1021/la400951s](https://doi.org/10.1021/la400951s).
- Bonaccorsi, L., Lombardo, D., Longo, A., Proverbio, E., and Triolo, A. (2009). “Dendrimer template directed self-assembly during zeolite formation”. *Macromolecules* **42**, 1239–1243. DOI: [10.1021/ma802393e](https://doi.org/10.1021/ma802393e).
- Caccamo, M. T., Cannuli, A., Calabrò, E., and Magazù, S. (2017). “Acoustic Levitator Power Device: Study of Ethylene-Glycol Water Mixtures”. *Journal of Physics: Conference Series* **199**(1), 012119. DOI: [10.1088/1757-899X/199/1/012119](https://doi.org/10.1088/1757-899X/199/1/012119).
- Caccamo, M. T. and Magazù, S. (2017a). “Multiscaling wavelet analysis of infrared and Raman data on polyethylene glycol 1000 aqueous solutions”. *Spectroscopy Letters* **50**(3), 130–136. DOI: [10.1080/00387010.2017.1291524](https://doi.org/10.1080/00387010.2017.1291524).
- Caccamo, M. T. and Magazù, S. (2017b). “Thermal restraint on PEG-EG mixtures by FTIR investigations and wavelet cross-correlation analysis”. *Polymer Testing* **62**, 311–318. DOI: [10.1016/j.polymertesting.2017.07.008](https://doi.org/10.1016/j.polymertesting.2017.07.008).
- Caccamo, M. T. and Magazù, S. (2019). “A physical-mathematical approach to climate change effects through stochastic resonance”. *Climate* **7**, 21. DOI: [10.3390/cli7020021](https://doi.org/10.3390/cli7020021).
- Caccamo, M. T. and Magazù, S. (2023). “Exponential feedback effects in a parametric resonance climate model”. *Sci Rep* **13**, 22984. DOI: [10.1038/s41598-023-50350-7](https://doi.org/10.1038/s41598-023-50350-7).
- Caccamo, M. T., Mavilia, G., Mavilia, L., Lombardo, D., and Magazù, S. (2020). “Self-assembly processes in hydrated montmorillonite by FTIR investigations”. *Materials* **13**, 1100. DOI: [10.3390/ma13051100](https://doi.org/10.3390/ma13051100).
- Castorina, G., Caccamo, M. T., Colombo, F., and Magazù, S. (2021). “The role of physical parameterizations on the numerical weather prediction: Impact of different cumulus schemes on weather forecasting on complex orographic areas”. *Atmosphere* **12**(5), 616. DOI: [10.3390/atmos12050616](https://doi.org/10.3390/atmos12050616).
- Castorina, G., Caccamo, M. T., Insinga, V., Magazù, S., Munaò, G., Ortega, C., Semprebello, A., and Rizza, U. (2022). “Impact of the Different Grid Resolutions of the WRF Model for the Forecasting of the Flood Event of 15 July 2020 in Palermo (Italy)”. *Atmosphere* **13**, 1717. DOI: [10.3390/atmos13101717](https://doi.org/10.3390/atmos13101717).
- Castorina, G., Caccamo, M. T., and Magazù, S. (2019). “Study of convective motions and analysis of the impact of physical parametrization on the wrf-arw forecast model”. *Atti della Accademia Peloritana dei Pericolanti. Classe di Scienze Fisiche, Matematiche e Naturali* **97**, A19. DOI: [10.1478/AAPP.97S2A19](https://doi.org/10.1478/AAPP.97S2A19).
- Chen, C., Wylie, R. A. L., Klinger, D., and Connal, L. A. (2017). “Shape Control of Soft Nanoparticles and Their Assemblies”. *Chemistry of Materials* **29** (5), 1918–1945. DOI: [10.1021/acs.chemmater.6b04700](https://doi.org/10.1021/acs.chemmater.6b04700).
- Chen, S., Mallamace, F., Faraone, A., Gambadauro, P., Lombardo, D., and Chen, W. (2002). “Observation of a re-entrant kinetic glass transition in a micellar system with temperature-dependent attractive interaction”. *The European Physical Journal E* **9**, 283–286. DOI: [10.1140/epje/i2002-10081-5](https://doi.org/10.1140/epje/i2002-10081-5).
- Colomban, P. and Slodczyk, A. (2010). “Raman Intensity: An Important Tool in the Study of Nanomaterials and Nanostructures”. *Acta Physica Polonica A* **116**, 7–12. DOI: [10.12693/APhysPolA.116.7](https://doi.org/10.12693/APhysPolA.116.7).

- Fan, L. and Bao, Y. (2021). “Review of fiber optic sensors for corrosion monitoring in reinforced concrete”. *Cement and Concrete Composites* **120**, 104029. DOI: [10.1016/j.cemconcomp.2021.104029](https://doi.org/10.1016/j.cemconcomp.2021.104029).
- Faraone, A., Magazù, S., Maisano, G., Ponterio, R., and Villari, R. (1999). “Experimental Evidence of Slow Dynamics in Semidilute Polymer Solutions”. *Macromolecules* **32**(4), 1128–1133. DOI: [10.1021/ma9809684](https://doi.org/10.1021/ma9809684).
- Gastaldi, D., Canonico, F., Irico, S., and al., et (2010). “Near-infrared spectroscopy investigation on the hydration degree of a cement paste”. *Journal of Materials Science* **45**, 3169–3174. DOI: [10.1007/s10853-010-4323-9](https://doi.org/10.1007/s10853-010-4323-9).
- Geiker, M. R., Hendriks, M. A. N., and Elsener, B. (2023). “Durability-based design: the European perspective”. *Sustainable and Resilient Infrastructure* **8**, 169–184. DOI: [10.1080/23789689.2021.1951079](https://doi.org/10.1080/23789689.2021.1951079).
- Gierlinger, N. and Schwanninger, M. (2007). “The potential of Raman microscopy”. *Spectroscopy* **21**, 69–89. DOI: [10.1155/2007/498206](https://doi.org/10.1155/2007/498206).
- Gordon, M. S., Smith, Q. A., Xu, P., and Slipchenko, L. V. (2013). “Accurate First Principles Model Potentials for Intermolecular Interactions”. *Annual Review of Physical Chemistry* **64**, 553–578. DOI: [10.1146/annurev-physchem-040412-110031](https://doi.org/10.1146/annurev-physchem-040412-110031).
- Hidalgo, A., Domingo, C., Garcia, C., Petit, S., Andrade, C., and Alonso, C. (2008). “Microstructural changes induced in Portland cement-based materials due to natural and supercritical carbonation”. *Journal of Materials Science* **43**, 3101–3111. DOI: [10.1007/s10853-008-2521-5](https://doi.org/10.1007/s10853-008-2521-5).
- Higl, J., Hinder, D., Rathgeber, C., Ramming, B., and Lindén, M. (2021). “Detailed in situ ATR-FTIR spectroscopy study of the early stages of C-S-H formation during hydration of monoclinic C3S”. *Cement and Concrete Research* **142**, 106367. DOI: [10.1016/j.cemconres.2021.106367](https://doi.org/10.1016/j.cemconres.2021.106367).
- Irassar, F. E., Bonavetti, V. L., and González, M. (2003). “Microstructural study of sulfate attack on ordinary and limestone Portland cements at ambient temperature”. *Cement and Concrete Research* **33**, 31–41. DOI: [10.1016/S0008-8846\(02\)00914-6](https://doi.org/10.1016/S0008-8846(02)00914-6).
- Jose, A., Nivitha, M. R., Krishnan, J. M., and Robinson, R. G. (2020). “Characterization of cement stabilized pond ash using FTIR spectroscopy”. *Construction and Building Materials* **263**, 120136. DOI: [10.1016/j.conbuildmat.2020.120136](https://doi.org/10.1016/j.conbuildmat.2020.120136).
- Jouzel, J., Lorius, C., Petit, J., and al., et (1987). “Vostok ice core: a continuous isotope temperature record over the last climatic cycle (160,000 dates)”. *Nature* **329**, 403–408. DOI: [10.1038/329403a0](https://doi.org/10.1038/329403a0).
- Lacasse, M. A., Gaur, A., and Moore, T. V. (2020). “Durability and Climate Change—Implications for Service Life Prediction and the Maintainability of Buildings”. *Buildings* **10**, 53. DOI: [10.3390/buildings10030053](https://doi.org/10.3390/buildings10030053).
- Lee, Y. S. (2008). *Self-Assembly and Nanotechnology, a Force Balance Approach*. Hoboken, NJ, USA: John Wiley & Sons, Inc.
- Lombardo, D. (2009). “Liquid-like ordering of negatively charged poly(amidoamine) (PAMAM) dendrimers in solution”. *Langmuir* **25**(5), 3271–3275. DOI: [10.1021/la804234p](https://doi.org/10.1021/la804234p).
- Lombardo, D., Calandra, P., Caccamo, M. T., Magazù, S., and Kiselev, M. A. (2019). “Colloidal stability of liposomes”. *American Institute of Mathematical Sciences Materials Science* **6** (2), 200–213. DOI: [10.3934/mat.2019.2.200](https://doi.org/10.3934/mat.2019.2.200).
- Lombardo, D., Calandra, P., and Kiselev, M. A. (2020). “Structural characterization of biomaterials by means of small angle X-rays and neutron scattering (SAXS and SANS), and light scattering experiments”. *Molecules* **25**, 5624. DOI: [10.3390/molecules25235624](https://doi.org/10.3390/molecules25235624).
- Long, D. (1977). *Raman Spectroscopy*. New York: McGraw-Hill International Book Company.
- Magazù, S. and Caccamo, M. (2022). “Climate Change Dynamics and Modeling: Future Perspectives”. *Climate* **10**, 65. DOI: [10.3390/cli10050065](https://doi.org/10.3390/cli10050065).

- Magazù, S., Maisano, G., Mallamace, F., and Micali, N. (1989). “Growth of fractal aggregates in water solutions of macromolecules by light scattering”. *Physical Review A* **39**, 4195–4200. DOI: [10.1103/PhysRevA.39.4195](https://doi.org/10.1103/PhysRevA.39.4195).
- Magazù, S., Migliardo, F., and Benedetto, A. (2011). “Elastic incoherent neutron scattering operating by varying instrumental energy resolution: principle, simulations, and experiments of the resolution elastic neutron scattering (RENS)”. *Review of Scientific Instruments* **82**(10), 105115. DOI: [10.1063/1.3641870](https://doi.org/10.1063/1.3641870).
- Magazù, S., Migliardo, F., Benedetto, A., Calabrò, E., La Torre, R., and Caccamo, M. T. (2013). “Bioprotective Effects of Sucrose and Trehalose on Proteins”. In: *Sucrose: Properties, Biosynthesis and Health Implications*. Nova Science Publishers. Chap. 2.
- Martinez-Ramirez, S. and Fernandez-Carrasco, L. (2010). *Raman Spectroscopy: Application to Cementitious Systems*. Nova Science Publisher.
- Martinez-Ramirez, S., Sanchez-Cortes, S., Garcia-Ramos, J. V., Domingo, C., Fortes, C., and Blanco-Varela, M. T. (2003). “Micro-Raman spectroscopy applied to depth profiles of carbonates formed in lime mortar”. *Cement and Concrete Research* **33**, 2063–2068. DOI: [10.1016/S0008-8846\(03\)00227-8](https://doi.org/10.1016/S0008-8846(03)00227-8).
- Masmoudi, R., Kupwade-Patil, K., Bumajdad, A., and Büyükoztürk, O. (2017). “In situ Raman studies on cement paste prepared with natural pozzolanic volcanic ash and Ordinary Portland Cement”. *Construction and Building Materials* **148**, 444–454. DOI: [10.1016/j.conbuildmat.2017.05.016](https://doi.org/10.1016/j.conbuildmat.2017.05.016).
- Micali, N., Scolaro, L. M., Romeo, A., Lombardo, D., Lesieur, P., and Mallamace, F. (1998). “Structural properties of methanol-polyamidoamine dendrimer solutions”. *Physical Review E* **58**(5), 6229. DOI: [10.1103/PhysRevE.58.6229](https://doi.org/10.1103/PhysRevE.58.6229).
- Narayanan, T. and Konovalov, O. (2020). “Synchrotron Scattering Methods for Nanomaterials and Soft Matter Research”. *Materials* **13**(3), 752. DOI: [10.3390/ma13030752](https://doi.org/10.3390/ma13030752).
- Neville, A. (1995). *Properties of Concrete*. Fifth. San Francisco: Prentice Hall.
- Qu, F. L., Li, W. G., Dong, W. K., Tam, V. W. Y., and Yu, T. (2021). “Durability deterioration of concrete under marine environment from material to structure: A critical review”. *Journal of Building Engineering* **35**, 102074. DOI: [10.1016/j.jobbe.2020.102074](https://doi.org/10.1016/j.jobbe.2020.102074).
- Robles, K. P. V., Yee, J. J., and Kee, S. H. (2022). “Electrical Resistivity Measurements for Non-destructive Evaluation of Chloride-Induced Deterioration of Reinforced Concrete—A Review”. *Materials* **15**, 2725. DOI: [10.3390/ma15082725](https://doi.org/10.3390/ma15082725).
- Rodrigues, R., Gaboreau, S., Gance, J., Ignatiadis, I., and Betelu, S. (2021). “Reinforced concrete structures: A review of corrosion mechanisms and advances in electrical methods for corrosion monitoring”. *Construction and Building Materials* **269**, 121240. DOI: [10.1016/j.conbuildmat.2020.121240](https://doi.org/10.1016/j.conbuildmat.2020.121240).
- Rouainia, M., Helm, P., Davies, O., and al., et (2020). “Deterioration of an infrastructure cutting subjected to climate change”. *Acta Geotech* **15**, 2997–3016. DOI: [10.1007/s11440-020-00965-1](https://doi.org/10.1007/s11440-020-00965-1).
- Sahu, S., Exline, D. L., and Nelson, M. P. (2002). “Identification of thaumasite in concrete by Raman chemical imaging”. *Cement and Concrete Composites* **24**, 347–350. DOI: [10.1016/S0958-9465\(01\)00086-5](https://doi.org/10.1016/S0958-9465(01)00086-5).
- Saillio, M., Baroghel-Bouny, V., Pradelle, S., Bertin, M., Vincent, J., and Lacaillerie, J.-B. d’Espinose de (2021). “Effect of supplementary cementitious materials on carbonation of cement pastes”. *Cement and Concrete Research* **142**, 106358. DOI: [10.1016/j.cemconres.2021.106358](https://doi.org/10.1016/j.cemconres.2021.106358).
- Ševčík, R. and Mácová, P. (2018). “Localized quantification of anhydrous calcium carbonate polymorphs using micro-Raman spectroscopy”. *Vibrational Spectroscopy* **95**, 1–6. DOI: [10.1016/j.vibspec.2017.12.005](https://doi.org/10.1016/j.vibspec.2017.12.005).
- Shevtsov, D., Cao, N. L., Nguyen, V. C., Nong, Q. Q., Le, H. Q., Nguyen, D. A., Zartsyn, I., and Kozaderov, O. (2022). “Progress in Sensors for Monitoring Reinforcement Corrosion in Reinforced Concrete Structures—A Review”. *Sensors* **22**, 3421. DOI: [10.3390/s22093421](https://doi.org/10.3390/s22093421).

- Shi, Z., Geng, G., Leemann, A., and Lothenbach, B. (2019). "Synthesis, characterization, and water uptake property of alkali-silica reaction products". *Cement and Concrete Research* **121**, 58–71. DOI: [10.1016/j.cemconres.2019.04.009](https://doi.org/10.1016/j.cemconres.2019.04.009).
- Simonpietro, A. (2021). *Spectroscopy for Materials Characterization*. John Wiley & Sons, Inc. DOI: [10.1002/9781119698029](https://doi.org/10.1002/9781119698029).
- Skocek, J., Zajac, M., and Ben Haha, M. (2020). "Carbon Capture and Utilization by mineralization of cement pastes derived from recycled concrete". *Scientific Reports* **10**, 5614. DOI: [10.1038/s41598-020-62503-z](https://doi.org/10.1038/s41598-020-62503-z).
- Tang, C., Ling, T.-C., and Mo, K. H. (2021). "Raman spectroscopy as a tool to understand the mechanism of concrete durability—A review". *Construction and Building Materials* **268**, 121079. DOI: [10.1016/j.conbuildmat.2020.121079](https://doi.org/10.1016/j.conbuildmat.2020.121079).
- Thakur, A. (2022). "Structural Health Monitoring Through the Application of Piezoelectric Sensors—State of the Art Review". *Advances in Construction Materials and Sustainable Environment* **196**, 657–673. DOI: [10.1007/978-981-16-6557-8\\_54](https://doi.org/10.1007/978-981-16-6557-8_54).
- Valliant, E. M., Dickey, B. T., Price, R., Boyd, D., and Filiaggi, M. J. (2016). "Fourier transform infrared spectroscopy as a tool to study the setting reaction in glass-ionomer cements". *Materials Letters* **185**, 256–259. DOI: [10.1016/j.matlet.2016.08.131](https://doi.org/10.1016/j.matlet.2016.08.131).
- Wagatsuma, K. (2021). *Spectroscopy for Materials Analysis*. Springer Singapore. DOI: [10.1007/978-981-16-5946-1](https://doi.org/10.1007/978-981-16-5946-1).
- Yoon, I. S., Copuroglu, O., and Ki-Bong, P. (2007). "Effect of global climatic change on carbonation progress of concrete". *Atmospheric Environment* **41**, 7274–7285. DOI: [10.1016/j.atmosenv.2007.05.028](https://doi.org/10.1016/j.atmosenv.2007.05.028).
- Yue, Y., Bai, Y., Muhammed Basheer, P. A., Boland, J. J., and Wang, J. J. (2013). "Monitoring the cementitious materials subjected to sulfate attack with optical fiber excitation Raman spectroscopy". *Optical Engineering* **52**, 104107. DOI: [10.1117/1.OE.52.10.104107](https://doi.org/10.1117/1.OE.52.10.104107).
- Yue, Y., Wang, J. J., Basheer, P. A. M., Boland, J. J., and Bai, Y. (2018). "A Raman spectroscopy based optical fibre system for detecting carbonation profile of cementitious materials". *Sensors and Actuators B: Chemical* **257**, 635–649. DOI: [10.1016/j.snb.2017.10.160](https://doi.org/10.1016/j.snb.2017.10.160).
- Zemb, T. and Lindner, P. (2002). *Neutron, X-rays and Light Scattering Methods Applied to Soft Condensed Matter*. Amsterdam, The Netherlands: North-Holland Elsevier.
- Zhan, B. J., Xuan, D. X., Poon, C. S., Shi, C. J., and Kou, S. C. (2018). "Characterization of C-S-H formed in coupled CO<sub>2</sub>-water cured Portland cement pastes". *Materials and Structures* **51**, 92. DOI: [10.1617/s11527-018-1211-2](https://doi.org/10.1617/s11527-018-1211-2).

- 
- <sup>a</sup> Consiglio Nazionale delle Ricerche  
Istituto per i Processi Chimico-Fisici  
Viale F. Stagno d'Alcontres, 37, 98158 Messina, Italy
- <sup>b</sup> Università degli Studi di Messina,  
Dipartimento di Scienze Matematiche e Informatiche, Scienze Fisiche e Scienze della Terra,  
Viale F. Stagno d'Alcontres, 31, 98166 Messina, Italy
- <sup>c</sup> Consorzio Interuniversitario Scienze Fisiche Applicate (CISFA),  
Viale F. Stagno d'Alcontres, 31, 98166 Messina, Italy
- <sup>d</sup> Istituto Nazionale di Geofisica e Vulcanologia (INGV)  
Sezione di Palermo, Sede Operativa di Milazzo  
Via dei Mille, 98057 Milazzo, Messina, Italy
- \* To whom correspondence should be addressed | email: lombardo@ipcf.cnr.it

Paper contributed to the international conference on  
"Atmospheric Monitoring, Modeling and Simulation", held in Messina, Italy (2-3 December 2019)  
under the patronage of the *Accademia Peloritana dei Pericolanti*

Manuscript received 6 October 2023; published online 1 October 2025



© 2025 by the author(s); licensee *Accademia Peloritana dei Pericolanti* (Messina, Italy). This article is an open access article distributed under the terms and conditions of the [Creative Commons Attribution 4.0 International License](https://creativecommons.org/licenses/by/4.0/) (<https://creativecommons.org/licenses/by/4.0/>).